

## New Dissociation Channels in D<sub>2</sub>O

J. Derbyshire, W. Kedzierski, and J. W. McConkey

*Department of Physics, University of Windsor, Windsor, Ontario N9B 3P4, Canada*

(Received 7 April 1997; revised manuscript received 15 July 1997)

Making use of a novel solid xenon matrix detector which is selectively sensitive to O(<sup>1</sup>S<sub>0</sub>) metastable atoms, a new dissociation channel, via a <sup>1</sup>A<sub>1</sub> repulsive state, has been uniquely identified following electron impact on D<sub>2</sub>O molecules. Careful measurements of the O fragment kinetic energies and appearance potentials have allowed partial reconstruction of the potential energy surface involved. The excitation function for production of O(<sup>1</sup>S<sub>0</sub>) has a shape which is characteristic of an optically allowed transition in the parent molecule and has a maximum value of  $1.2 \times 10^{-18}$  cm<sup>2</sup> at 100 eV incident electron energy. [S0031-9007(97)04081-7]

PACS numbers: 34.80.Gs

Fragments from the dissociation of water are minor species in our atmosphere but play an inordinately important role in its chemistry [1]. Further, the dissociation of water is of great interest in studies of space physics and radiation chemistry [2,3]. Thus the fragmentation of water continues to be a fertile ground for study.

The early photoabsorption work of Watanabe and Zelikoff [4] revealed the existence of two broad continua representing excitation of the *A* and *B* repulsive states of the parent molecule and leading to production of ground state H atoms and OH molecules in the X<sup>2</sup>Π and A<sup>2</sup>Σ<sup>+</sup> states, respectively. Use of laser techniques enabled Andresen *et al.* [5] and others to make very specific and detailed state to state studies which have led to a major elucidation of the photodissociation dynamics, at least for these relatively low-lying states. Brouard *et al.* [6] give an update of this work and give extensive references to earlier work. Synchrotron radiation has also been widely exploited to study the production of excited fragments, usually by monitoring the fluorescence or ionization which occurs. Using these techniques Wu and Judge [7] have monitored these fragmentation processes to photon energies of 20.5 eV and discuss a wide range of fragmentation channels.

Significant information relevant to dissociation mechanisms has also been obtained from studies of electron or photon irradiation of water in the condensed phase [8]. Techniques such as laser resonance enhanced multiphoton ionization (REMPI) have been used to probe the fragments desorbed from the water surface.

Electron impact gas phase work has involved metastable fragment production [9,10], nonmetastable excited fragment production [11–13], and dissociative ionization and attachment [14]. A wide range of techniques has been applied including laser induced fluorescence to probe the production of unexcited fragments [15,16], and Doppler broadening of emission lines to reveal fragment kinetic energies [17,18].

Electron impact techniques have the advantage over photon impact in that optically and spin forbidden excitation channels can be probed. However, this has a down-

side as well in that it often leads to ambiguities in seeking to define the dissociation dynamics. This occurs because a particular fragment may be produced via a number of overlapping mechanisms.

In the present work we take advantage of a novel detector which is selectively sensitive to O(<sup>1</sup>S) in order to probe a subset of dissociation mechanisms. Further, by directly measuring fragment energies and appearance potentials, we are able to probe specific fragmentation channels in the Franck-Condon region.

The apparatus has been described previously [19,20], and so only a brief summary will be given here. A crossed-beam arrangement is used in which the magnetically collimated electron beam and the target water beam are mutually orthogonal. The water molecules effuse from a capillary tube, and a capacitance manometer is used to monitor the driving pressure (typically 5–10 torr) upstream of this tube. The detector is located 27 cm from the interaction region in the direction of the molecular beam. It consists of an approximately 1 mm thick layer of solid xenon which is grown on a cold finger at 69 K in a second differentially pumped chamber. A small steady flow of xenon into this chamber keeps the background pressure at approximately  $2 \times 10^{-4}$  torr and continuously refreshes the layer on the cold finger. The Xe layer lies in the field of view of a cooled photomultiplier with a GaAs photocathode. A Plexiglas light pipe between the Xe layer and the photomultiplier enhances the aperture of the detection system. Filters can be placed in the optical path as required. The electron beam was pulsed and a time-to-amplitude convertor (TAC) was used to acquire time-of-flight (TOF) spectra. Alternatively time-of-flight windows could be chosen and the electron energy varied under computer control so that excitation functions, appropriate to data arriving at the detector during that window, could be obtained.

The operation of the xenon layer detector has been explained earlier, but a brief summary is as follows. O(<sup>1</sup>S) atoms impact the Xe surface, thermalize, and form excimers within a few microseconds. The XeO state which

is formed has a radiative lifetime of about 100 ns. The resulting emission occurs in two broad bands centered at 725 and 375 nm, respectively, in order of decreasing intensity. In this experiment flight times to the detector were typically 100  $\mu$ s, and so the thermalization and radiative lifetimes were negligible in comparison. Key characteristics of the detector are its sensitivity [quantum efficiency close to unity for  $O(^1S)$ ] and its extreme selectivity. It is totally insensitive to all other fragments produced in the electron- $D_2O$  interaction. Thus it allows a very selective probing of the multitude of dissociation curves along which the molecule may fragment. An isotropic distribution of fragments from the dissociation process is assumed.

Figure 1 shows TOF data for  $D_2O$  fragmentation taken at 40 eV impact energy. At very short times the signal is dominated by photons which reach the detector directly from the interaction region during the exciting electron pulse. After that a single peak is observed with a maximum occurring at a flight time of 120  $\mu$ s and with a long tail to longer flight times. At higher (lower) incident energies, the leading edge of the TOF distribution is shifted slightly to shorter (longer) flight times and the full width at half maximum (FWHM) of the peak narrows (broadens) by a few percent. Some data have also been taken with  $H_2O$  targets, and here the peak is observed to be 10% broader (FWHM) and to occur at slightly longer times than in the case of  $D_2O$  (130 rather than 110  $\mu$ s at 100 eV incident energy). This reflects the fact that, although the repulsive curves and hence the total released kinetic energy for the two molecules must be the same, the sharing of the released kinetic energy between the different fragments depends on their respective masses. Simple momentum considerations show that  $O(^1S)$  from  $D_2O$  should be more energetic.

A slight shoulder was consistently observed at flight times less than 100  $\mu$ s. This, together with the changes in

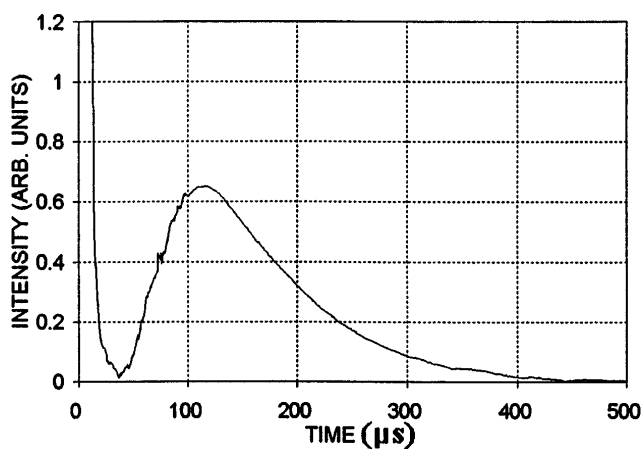


FIG. 1. Time-of-flight spectrum for  $O(^1S)$  fragments obtained at an incident electron energy of 40 eV. Zero time corresponds to the center of the 20  $\mu$ s wide electron pulse. Some smoothing has been applied to reduce the statistical scatter in the data.

the distribution as the incident electron energy is changed, suggests that more than one channel contribute to the production of  $O(^1S)$  fragments, particularly as the impact energy is increased.

Knowing the identity of the detected particle, it is readily possible to convert the 40 eV TOF data in Fig. 1 to a kinetic energy spectrum, Fig. 2 (see Ref. [19] for details). The accuracy in the conversion process is reduced at the lowest energies (longest flight times) due to the small signals and the  $t^3$  factor which is involved. Kinematic effects could also occur at energies close to the thermal energy (25 meV) of the parent beam. For these reasons, data at the very lowest energies have been suppressed. The distribution peaks at 0.2 eV but has a long tail stretching to about 3 eV. At 30 eV impact energy the width of the distribution is reduced from 0.6 to 0.46 eV, FWHM, and the peak position occurs at about 0.15 eV. Again this suggests that additional production channels open up as the energy of the incident electrons is increased. The peak occurs at a lower energy and has a narrower half-width for  $H_2O$  targets.

Figure 3 shows the excitation function for  $O(^1S)$  production from  $D_2O$  over the energy range 0–320 eV. Care was taken to ensure that the complete  $O(^1S)$  TOF spectrum was included in the acceptance window of the detector at all incident energies. The curve rises steeply from threshold around 15.3 eV to a broad maximum in the 100 eV region. This shape is characteristic of optically allowed transitions in the parent molecule. To establish the threshold energy, comparison was made with the threshold for production of prompt photons (predominantly Balmer- $\alpha$  [21]). In both cases the thresholds were taken as the points where the initial linear rise of the excitation function was extrapolated back to cut the energy axis. The Balmer- $\alpha$  threshold was taken as 18.25 eV, the average of the two values quoted by Beenakker *et al.* [21]. Since the uncertainty in this figure is 0.5 eV, our threshold energy is uncertain by approximately this amount also. If another

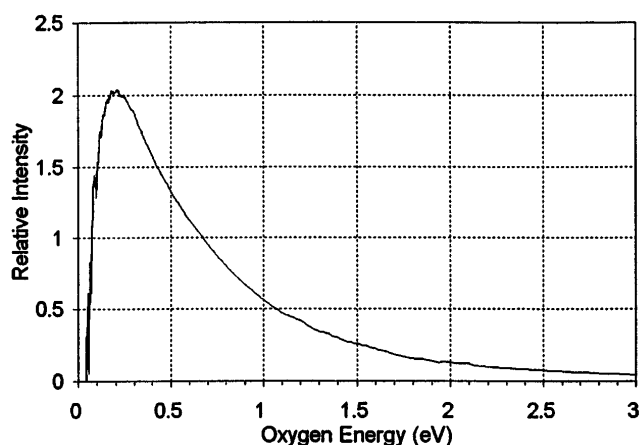


FIG. 2.  $O(^1S)$  fragment kinetic energy spectrum obtained from the data in Fig. 1.

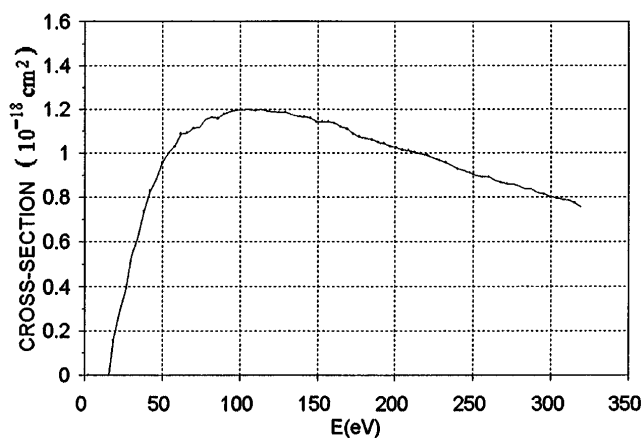
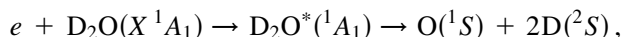


FIG. 3. Absolute cross section for the production of  $O(^1S)$  following electron impact on  $D_2O$ . The data have been normalized as discussed in the text. Some smoothing has been applied to reduce the statistical scatter in the data.

process was occurring with a lower threshold energy, its cross section must be less than  $2 \times 10^{-20} \text{ cm}^2$  in this energy region, i.e., insignificant relative to the process being observed here.

Knowing the threshold energy for the process, the fact that one of the products is  $O(^1S)$ , and the energy released as kinetic energy (approximately 1–2 eV based on simple conservation of momentum considerations), allows us to estimate the energy at infinite separation, namely, 13.3–14.3 eV. We make the reasonable assumption here that the two D fragments leave the collision complex separately and symmetrically at angles greater than  $135^\circ$  to the O fragment direction, i.e., essentially in the opposite direction to the O fragment. As mentioned later, dissociation via a bending vibration seems to be the most reasonable breakup mechanism.

The only possible fragmentation process which fits the observed energetics is



with a threshold energy of 13.82 eV. If one of the D atoms were to be excited, the threshold would be at least 10.2 eV higher in energy. Similarly, if the D atoms were united as a molecule the threshold energies would be 9.24 eV [for  $D_2(X)$ ] or 20.61 eV [for  $D_2(B)$ ]. Thus these channels can also be excluded as possibilities. We note that Theodorakopoulos *et al.* [22] have carried out *ab initio* calculations of the dissociation of  $H_2O$  into  $H_2$  and an oxygen fragment. Their work reveals that a significant (4 eV) barrier to dissociation into  $O(^1S) + H_2(X)$  exists. This would increase the threshold energy for  $O(^1S) + D_2(X)$  production to approximately 13.2 eV. This is still 2 eV below what we observe.

Because the dissociation products are so well defined and because the shape of the excitation function indicates that no spin change occurs in the excitation process to the parent repulsive state, this parent state can be un-

ambiguously classified, using the procedure outlined by Herzberg [23], as having  $^1A_1$  character. Wu and Judge [7] show some minor structure at a photon energy of 15.3 eV (80.9 nm) on their curves showing neutral particle production following photoabsorption by  $H_2O$ . This could be identified with  $O(^1S)$  production.

We note further that little can be said about the other channels which open up at higher incident energies, except to conclude, from the absence of sharp structure on the excitation function (Fig. 3), that these parent states must be of singlet character also. There is consistent evidence for a slight shoulder on the excitation functions at around 10 eV above threshold (barely observable on Fig. 3). We note that this would be consistent with total fragmentation of the parent molecule and excitation of one of the D atoms to the  $n = 2$  state. Direct observation of H ( $n = 2$ ) following electron impact on  $H_2O$  by various groups [24–27] clearly demonstrates the opening up of a production channel at about 25 eV. This would be consistent with the suggested mechanism given above.

The cross-section data in Fig. 3 have been made absolute by comparing the signals obtained from  $D_2O$  targets with those obtained from  $CO_2$  under the same conditions of excitation (electron beam current, target gas pressure, etc.). A  $CO_2$  cross section of  $1.56 \times 10^{-17} \text{ cm}^2$  at 100 eV was used for normalization [20]. There are a number of sources of uncertainty in this procedure. First, there is a lack of detailed knowledge of how the sensitivity of the detector depends on impinging O-atom velocity. Since thermalization of the  $O(^1S)$  atoms occurs prior to excimer formation and since the range of fragment velocities is similar for the two molecular targets, the assumption of equal sensitivity for both is judged to be reasonable. Second, since the molecular masses are dissimilar, the two target beams may not be directly comparable. Third, variations in detector sensitivity, with such parameters as surface temperature, could occur over prolonged (24 h) data acquisition periods. A large number of comparisons were carried out at different beam driving pressures in order to minimize the effects of these problems. Assuming the quoted uncertainty of 12% in the calibration standard allows an overall uncertainty of 35% to be estimated.

The value obtained at 100 eV ( $1.2 \times 10^{-18} \text{ cm}^2$ ) is a factor of 16 less than the cross section for production of Lyman- $\alpha$  following electron impact dissociation of water by electrons of the same energy [27]. Considering the cross sections for production of other excited fragments [21] suggests that  $O(^1S)$  production accounts for about 5% of dissociation which produces excited fragments.

If we assume that a transition takes place vertically in the Franck-Condon region we can fix the parent repulsive surface in this region (at 15.3 eV above the ground state). Also, our knowledge of the nature, internal energy, etc., of the fragments allows us to fix the repulsive surface at infinite internuclear separations (at 13.82 eV above the  $D_2O$  ground state).

The uncertainty in the first of these numbers arises partly because of the uncertainty in our energy calibration, partly because TOF data of high statistical significance could not be obtained in the near threshold region and partly because the exact details of the dynamics of the total fragmentation process are unknown. It is reasonable to suppose that a bending vibration, in which the O atom and the two D atoms are ejected in approximately opposite directions, forms the basis of the breakup mechanism.

In conclusion, we have monitored the fragmentation of D<sub>2</sub>O where the O fragment is unambiguously O(<sup>1</sup>S). The energetics of the breakup near threshold allow the dominant parent repulsive state to be positively identified as <sup>1</sup>A<sub>1</sub>. The other fragments can only be ground state D atoms in this case. From the shape of the excitation cross section, essentially only singlet repulsive states are involved in O(<sup>1</sup>S) production. The total cross section involved indicates that these dissociation channels are non-negligible.

We are grateful to the Natural Sciences and Engineering Research Council of Canada for financial assistance and to the staff of the mechanical and electronic workshops at the University of Windsor for expert technical help.

- 
- [1] B. G. Levi, *Phys. Today* **49**, No. 11, 17 (1996).
  - [2] M. Singh, *Astrophys. Space Sci.* **141**, 75 (1988).
  - [3] J. J. Olivero, R. W. Stagat, and A. E. S. Green, *J. Geophys. Res.* **77**, 4797 (1972).
  - [4] K. Watanabe and M. Zelikoff, *J. Opt. Soc. Am.* **43**, 753 (1953).
  - [5] P. Andresen, G. S. Ondrey, B. Titze, and E. W. J. Rothe, *J. Chem. Phys.* **80**, 2548 (1984).
  - [6] M. Brouard, S. R. Langford, and D. E. Manolopoulos, *J. Chem. Phys.* **101**, 7458 (1994).
  - [7] C. Y. R. Wu and D. L. Judge, *J. Chem. Phys.* **89**, 6275 (1988).

- [8] G. A. Kimmel and T. M. Orlando, *Phys. Rev. Lett.* **75**, 2606 (1995); **77**, 3983 (1996).
- [9] R. S. Freund, *Chem. Phys. Lett.* **9**, 135 (1971).
- [10] R. S. Freund, in *Rydberg States of Atoms and Molecules*, edited by R. F. Stebbings and F. B. Dunning (Cambridge University Press, Cambridge, 1983).
- [11] U. Muller, Th. Babel, and G. Schulz, *Z. Phys. D* **25**, 167 (1993).
- [12] S. Trajmar, D. F. Register, and A. Chutjian, *Phys. Rep.* **97**, 219 (1983).
- [13] J. W. McConkey, Argonne National Laboratory Report No. ANL 84-28, 1984, p. 129.
- [14] T. D. Mark and G. H. Dunn, *Electron Impact Ionization* (Springer-Verlag, Vienna, 1985).
- [15] H. Kawazumi and T. Ogawa, *Chem. Phys.* **114**, 149 (1987).
- [16] M. Darrach and J. W. McConkey, *Chem. Phys. Lett.* **184**, 141 (1991).
- [17] N. Kouchi, K. Ito, Y. Hatano, N. Oda, and T. Tsuboi, *Chem. Phys.* **36**, 239 (1979).
- [18] T. Ogawa, N. Yonekura, M. Tsukada, S. Ihara, T. Yasuda, H. Tomura, K. Nakashima, and H. Kawazumi, *J. Phys. Chem.* **95**, 2788 (1991).
- [19] L. R. LeClair and J. W. McConkey, *J. Chem. Phys.* **99**, 4566 (1993).
- [20] L. R. LeClair and J. W. McConkey, *J. Phys. B* **27**, 4039 (1994).
- [21] C. I. M. Beenakker, F. J. De Heer, H. B. Krop, and G. R. Mohlmann, *Chem. Phys.* **6**, 445 (1974).
- [22] G. Theodorakopoulos, C. A. Nicolaides, R. J. Buenker, and S. D. Peyerimhoff, *Chem. Phys. Lett.* **89**, 164 (1982).
- [23] G. Herzberg, *Molecular Spectra and Molecular Structure* (Van Nostrand Co., Princeton, 1967), Vol. III.
- [24] N. Bose and W. Sroka, *Z. Naturforsch.* **26A**, 1491 (1971); **28A**, 22 (1973).
- [25] H. D. Morgan and J. E. Mentall, *J. Chem. Phys.* **60**, 4734 (1974).
- [26] J. W. McGowan, J. F. Williams, and D. A. Vroom, *Chem. Phys. Lett.* **3**, 614 (1969).
- [27] G. R. Mohlmann, K. H. Shima, and F. J. De Heer, *Chem. Phys.* **28**, 331 (1978).